Ionospheric and thermospheric storms at equatorial latitudes observed by CHAMP, ROCSAT, and DMSP

N. Balan,[1,2] J. Y. Liu,[1] Y. Otsuka,[3] S. Tulasi Ram,[4] and H. Lühr[5]

Received 2 June 2011; revised 31 October 2011; accepted 15 November 2011; published 20 January 2012.

[1] Analysis of the dayside electron density (Ne) and neutral mass density (N) at 400 km height measured by CHAMP during 12 intense geomagnetic storms in 2000–2004, and ion densities at 600 km and 840 km heights measured by ROCSAT and DMSP during a few of the intense storms, reveal some new aspects. Thermospheric storms (change of N) reach the equator within 1.5 to 3 hours from the main phase (MP) onset of intense storms having short and steady MPs. The responses of the equatorial ionosphere (at CHAMP) to both MPs and RPs (recovery phases) of the storms are generally opposite to those at higher latitudes. In addition to the known opposite responses during MPs, the analysis reveals that positive ionospheric storms develop at equatorial latitudes (within about ±15° magnetic latitudes) during daytime RPs, while conventional negative storms occur at higher latitudes. Ionospheric storms also extend to the topside ionosphere beyond 850 km height and are generally positive (at DMSP), especially during MPs. The positive storms around the equatorial ionospheric peak during RPs are interpreted in terms of the potential sources such as (1) zero or westward electric fields due to disturbance dynamo and/or prompt penetration, (2) plasma convergence due to the mechanical effects of storm-time equatorward neutral winds and waves, (3) increase of atomic oxygen density and decrease of molecular nitrogen density due to the downwelling effect of the winds, and (4) photoionization. The positive storms in the topside ionosphere during MPs involve the rapid upward drift of plasma due to eastward PPEFs, reduction in the downward diffusion of plasma along the field lines, and plasma convergence due to equatorward winds and waves.

Citation: Balan, N., J. Y. Liu, Y. Otsuka, S. Tulasi Ram, and H. Lühr (2012), Ionospheric and thermospheric storms at equatorial latitudes observed by CHAMP, ROCSAT, and DMSP, *J. Geophys. Res.*, *117*, A01313, doi:10.1029/2011JA016903.

1. Introduction

[2] The equatorial ionosphere has been known to exhibit several special features under magnetically quiet and active conditions due to the horizontal orientation of the geomagnetic field; for reviews, see *Rajaram* [1977] and *Rishbeth* [2000, and references therein]. The northward horizontal magnetic field combined with eastward horizontal electric field generates the equatorial plasma fountain [*Hanson and Moffett*, 1966] that leads to the special features.

[3] The plasma fountain becomes a super fountain [*Balan et al.*, 2009] in the dayside main phase (MP) of intense geomagnetic storms due to eastward prompt penetration electric fields (PPEFs) [*Kelley et al.*, 2004]. The super fountain results in a rapid rise of the ionospheric peak height (hmax) over the equator [e.g., *Batista et al.*, 1991; *Paznukhov et al.*, 2007; *Abdu et al.*, 2008; *Sreeja et al.*, 2009a], with a large reduction in F region electron density (Ne), peak electron density (Nmax) and total electron content (TEC) (or negative ionospheric storms at equatorial latitudes) [e.g., *Balan et al.*, 2009, 2011a, 2011b]; the TEC integrated even above CHAMP (400 km height) during the MP of the Halloween storms (30 October 2003) shows a significant decrease around the equator [*Mannucci et al.,* 2005] though the decrease in TEC is generally smaller than that in Nmax. Simultaneously, the eastward PPEFs in the presence of storm-time equatorward neutral winds and waves produce increases in Ne, Nmax and TEC (or positive ionospheric storms) at higher latitudes [e.g., *Prölss and Jung,* 1978; *Balan and Rao,* 1990; *Burns et al.*, 1995; *Sastri et al.*, 2000; *Mannucci et al.*, 2005; *Lin et al.*, 2005; *Vijaya Lekshmi et al.*, 2007; *Lu et al.*, 2008; *Balan et al.*, *2010*, 2011b]. In other words, the equatorial and higher latitude ionospheres in general undergo opposite responses during the MP of intense geomagnetic storms.

[4] The positive ionospheric storms at mid and low latitudes during MPs turn to conventional negative ionospheric storms during the recovery phase (RP) of the geomagnetic storms due mainly to the dominance of the chemical effects

[1]Institute of Space Science, National Central University, Chung-Li, Taiwan.
[2]Also at Control and Systems Engineering, University of Sheffield, Sheffield, UK.
[3]Solar-Terrestrial Environment Laboratory, Nagoya University, Nagoya, Japan.
[4]Research Institute for Sustainable Humanosphere, Kyoto University, Kyoto, Japan.
[5]GFZ German Research Centre for Geosciences, Potsdam, Germany.

0148-0227/12/2011JA016903

of the storm-time equatorward neutral winds [*Fuller Rowell et al.*, 1994; *Prölss,* 1995; *Mendillo and Narvaez* 2010]. However, what type of variation the equatorial ionosphere undergoes during the RPs of the geomagnetic storms is not yet clear though there have been some good case studies. For example, using Nmax data, *Pincheira et al.* [2002] reported the inhibition of daytime EIA in the Brazilian sector during the RP of an intense storm. *Sreeja et al.* [2009b] observed the inhibition of the daytime EIA in Nmax and TEC in the Indian sector during the RP of a moderate storm. *C. M. Huang et al.* [2010] reported the inhibition of the EIA in TEC close to sunset during the RP of two intense storms. These authors interpreted the inhibition of EIA in terms of daytime westward electric fields.

[5] Using the electron density (Ne) and neutral mass density (N) data at 400 km height measured by CHAMP [*Reigber et al.*, 2002] during 12 intense geomagnetic storms, the present paper reports that the electron density at equatorial latitudes generally increase (or positive ionospheric storms develop) during daytime RPs while conventional negative storms occur at higher latitudes (section 4); the center of the positive storms at CHAMP is found to vary within about $\pm 15°$ magnetic latitudes. The altitude extend of the ionospheric storms is investigated by including the ion density data at 600 km height measured by ROCSAT [*Su et al.*, 1999] and at 840 km height measured by DMSP F15 (section 5). The potential source mechanisms of the positive ionospheric storms are discussed (section 6).

2. Satellite Data

[6] CHAMP (Challenging Minisatellite Payload) was launched on 15 July 2000 into a near-circular orbit with an inclination of 87.3°, an initial altitude of 456 km and orbital period of ≈90 min. The precession rate of its orbital plane is 1.5°/day. The in situ air mass density N is effectively probed by a triaxial accelerometer, which yields estimate of N with an accuracy of 6×10^{-14} kg m^{-3} at a sampling rate of 0.1 Hz (Level 2 data) [*Reigber et al.*, 2002]. The in situ electron density Ne is measured using a planar Langmuir probe (PLP) every 15 s. The data are normalized to 400 km height as described by *Liu et al.* [2005]. Each satellite track varies by less than 5° in longitudes and 10 km in altitudes within $\pm 60°$ latitudes; these variations do not affect the results obtained below. The CHAMP data (Ne and N) though limited to a single height (400 km) are good to investigate thermospheric and ionospheric storms. *Liu and Lühr* [2005], *Sutton et al.* [2005], and *Lei et al.* [2010] reported neutral density enhancements of up to 200%, 400%, 800% and 400% with respect to the quiet time values during the intense storms of 29 and 30 October 2003, 20 November 2003, and 7–9 November 2004. Using the mass density (N) data during 30 intense geomagnetic storms ($Dst_{min} < -100$ nT), *Liu et al.* [2010] developed a linear model for the density variations during storms. The simple model predicts all storm-induced mass density variations at CHAMP altitude reasonably well especially if orbital averages are considered.

[7] ROCSAT-1 (FORMOSAT-1), the first scientific satellite of Taiwan, was launched on 27 January 1999; the mission ended in June 2004. The satellite was in a near circular orbit at 600 km altitude with an inclination of 35° and orbital period of ≈95 min [*Su et al.*, 1999]. The in situ ion density (equal to Ne) data measured using an onboard IPEI (Ionospheric Plasma and Electrodynamics Instrument) with a high sampling rate (up to 1 kHz, averaged at 1-second) [*Yeh et al.*, 1999; *Tulasi Ram et al.*, 2009] are used in the present study. The ion density data at 840 km height measured by DMSP-F15 (Defense Meteorological Satellite Program) spacecraft (fixed at 0910/2110 hrs) with an inclination of 98.9° are also used in the study.

3. Electric Field Data

[8] Following the eastward prompt penetration electric field (PPEF) in the dayside of intense MPs [e.g., *Rastogi*, 1977; *Kikuchi et al.*, 1978] the net electric field over the equator generally remains null or westward in the dayside for some period of the RPs due to westward penetration and/or disturbance dynamo [e.g., *Blanc and Richmond*, 1980; *Kelley et al.*, 2003; *Maruyama et al.*, 2005; *Fejer et al.*, 2007]. However, the equatorial F region electric field data, which is an important parameter for the present study, are not available for all storm periods. The F region vertical drift velocity is measured at Jicamarca during the intense storm on 09 November 2004 and derived from the equatorial electrojet (EEJ) strength during the intense storm on 8 November 2004 [*Fejer et al.*, 2007; *Balan et al.*, 2010]. *C. S. Huang et al.* [2010] reported the vertical drift velocities in the topside ionosphere over the equator measured by the DMSP F13 satellite at 18 LT during the intense storms on 31 March 2001 and 29–30 October 2003. These electric field data are used in the discussion.

4. CHAMP Observations

[9] Table 1 lists the characteristics of the 12 geomagnetic storms that include 1 triple storm, 2 double storms and 5 single storms. The main phases (MPs) of the storms last from about 4 hours to 18 hours, and recovery phases (RPs) last from 3 hours (due to re-intensification) to over 24 hours. For each storm, the latitude variations of the CHAMP data at selected equatorial crossing times of CHAMP during MP and RP are shown. The equatorial crossing times of CHAMP in UT (UT1, UT2, etc.) are given at the top of the figures. The corresponding magnetic local times (MLT1, MLT2, etc.) and geographic longitudes (GLOG1, GLOG2, etc.) are noted along the bottom axes. The storm-time data are also compared with the corresponding previous quiet day data (noted by Q, UTQ, GLONGQ and MLTQ). The quiet time data correspond mainly to the epoch of the RPs when positive ionospheric storms are observed at equatorial latitudes. However, to avoid complications, only one quiet-time curve (data) is shown in each plot of two or three storm-time curves. It may be noted that though the Ne data are available for all 12 storms, the N data are available only for 4 storms (1 triple storm and 1 single storm).

4.1. Storms on 29–31 October 2003

4.1.1. Ionospheric Storms

[10] A series of three geomagnetic storms occurred on 29–31 October 2003 when CHAMP was crossing the 13.2 MLT meridian (Table 1 and Figure 1). Figure 2 shows the latitude profiles of Ne at different epochs (times) of the geomagnetic

Table 1. Characteristics of Geomagnetic Storms

Day of Main Phase	Time of Main Phase Onset (UT)	Time of Peak Main Phase (UT)	Main Phase Duration (h)	Minimum Dst (nT)	Recovery Phase Duration (h)	CHAMP Crossing Time (MLT)
29 Oct 2003	7	11	4	−151	3	13.2
29 Oct 2003	14	1	11	−353	17	13.2
30 Oct 2003	18	23	5	−383	>24	13.2
20 Nov 2003	3	21	18	−422	>24	11.6
31 Mar 2001	4	9	5	−387	8	14.9
31 Mar 2001	17	22	5	−284	>24	14.9
10 Aug 2000	21	7	10	−106	19	11.9
12 Aug 2000	2	10	8	−253	>24	11.9
11 Apr 2001	16	24	8	−271	>24	14.0
5 Nov 2001	19	7	10	−292	>24	19.5
24 Nov 2001	7	17	10	−221	>24	17.6
7 Nov 2004	20	7	11	−373	>24	15.0

storms; the epochs are identified by the vertical lines in Figure 1. As shown by Figure 1 and Figure 2a (dashed curve 1 and dot-dashed curve Q), following the onset of the first MP, Ne around the equator decreases below quiet time levels and the EIA crests shift to about ±20° magnetic latitudes showing the development of negative ionospheric storms around the equator due to eastward PPEF [see *C. S. Huang et al.*, 2010]; simultaneously positive storms develop at and outside the EIA crests. By the end of the short MP, the Ne pattern reverses (Figure 2a, solid curve 2) with the development a Ne peak (or positive storm) around the equator.

[11] During the MP of the following super storm (Figure 1 and Table 1), compared to quiet time levels (Figure 2b, dot-dashed curve Q), deep negative storms in Ne develop around the equator with positive storms at higher latitudes centered at around ±30° (Figure 2b, dashed curve 3). During RP, Ne around the equator starts increasing (Figure 2b, thin solid curve 4) and exceeds quiet time levels or produces positive storms (Figure 2b, thick solid curve S) with conventional negative storms at higher latitudes. Before the super storm on 29 October recovered, the next super storm (on 30 October) occurred (Figure 1, Table 1). During MP, Ne is again depleted widely around the equator with strong positive storms at higher latitudes centered at ±30° (Figure 2c, dashed curve 5). During RP, with negative storms at higher latitudes, Ne around the equator increases with time (Figure 2c, solid curve 6), produces positive storms (Figure 2d, dashed curve 7), and recovers toward quiet time levels by the end of RP (Figure 2d, solid curve 8, dot-dashed curve Q). However, the positive storms during the RPs of the super storms (29–30 October 2003) are delayed due to the deep and wide depletions of the equatorial ionosphere during MPs and extension of the negative storms in the south to the equator during early RPs. The deepest and widest negative storm around the equator and strongest positive storms at higher latitudes observed during the MP of the Halloween storm on 30 October (Figure 2c, dashed curve 5) [see also *Mannucci et al.*, 2005] are interpreted in terms of impulsive responses due to high rate of energy input at high latitudes and strong eastward PPEF due to fast rate of change of Dst [*Balan et al.*, 2011b].

4.1.2. Thermospheric Storms

[12] The development of thermospheric storms (change of N) is found to be similar during all geomagnetic storms. As shown by the comparison of Figure 1 and Figure 3, N increases impulsively at high latitudes with the onset of the comparatively weak but short (first) MP without fluctuations

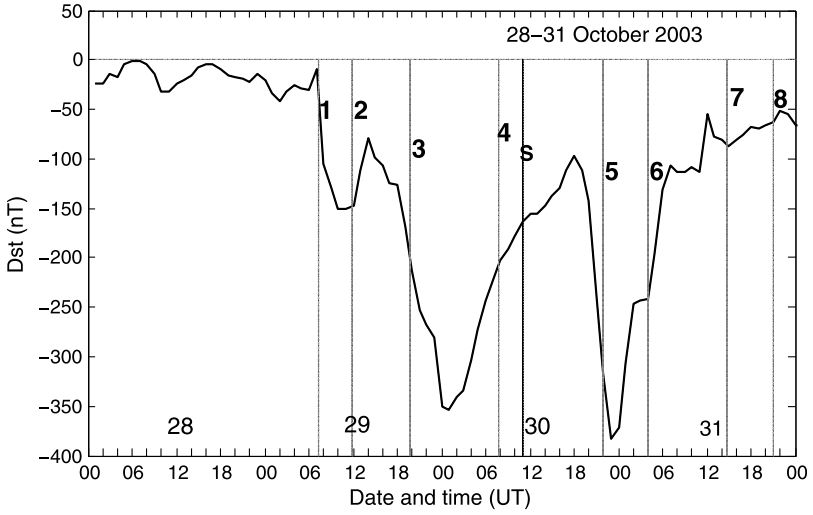

Figure 1. The triple geomagnetic storm of 29–31 October 2003; vertical lines represent the times when CHAMP data are shown in Figures 2 and 3.

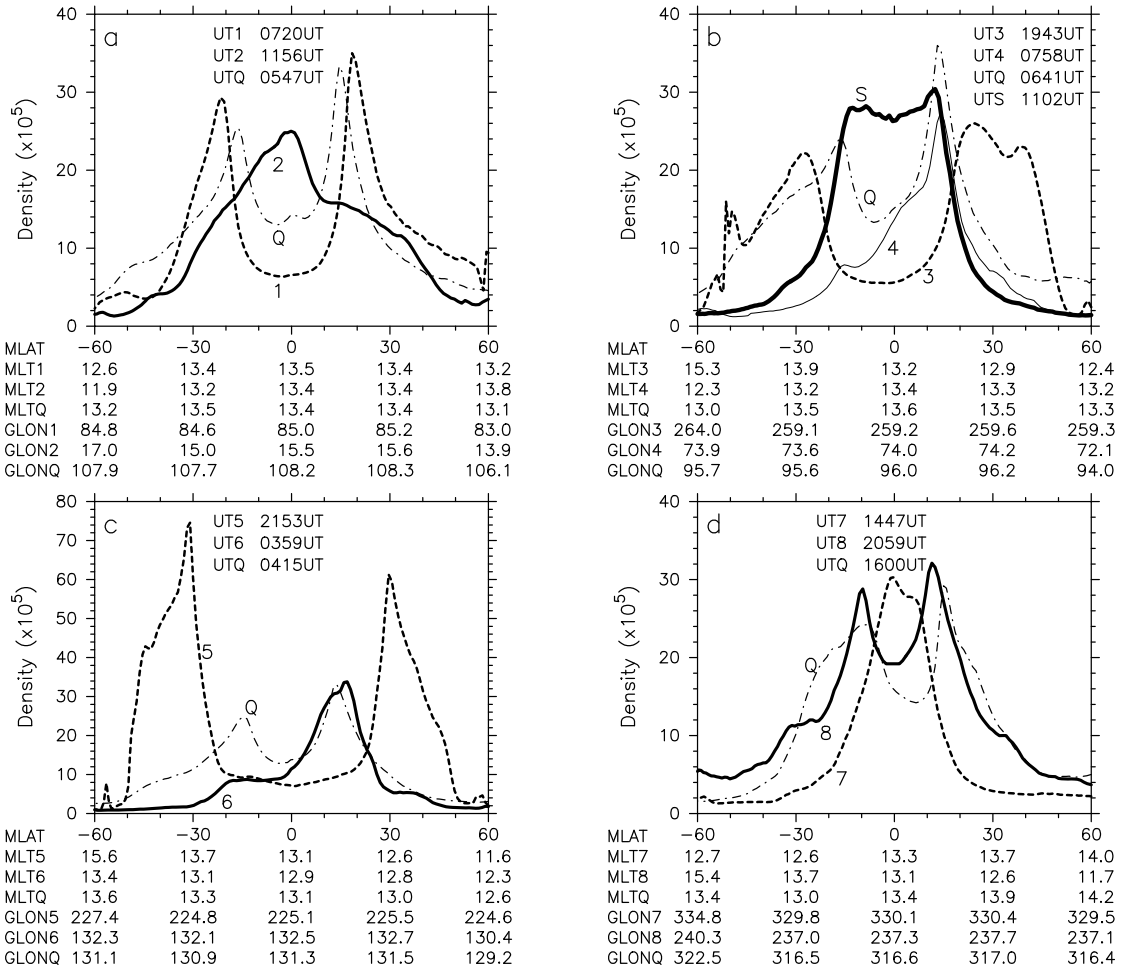

Figure 2. Latitude variations of the electron density Ne at selected equatorial crossing times of CHAMP during the triple storm of 29–31 October 2003. The satellite crossing times in UT (corresponding to the Ne plots) are noted at the top of each plot (and indicated by the vertical lines in Figure 1). The corresponding magnetic local times (MLTs) and geographic longitudes (GLOGs) are noted in the bottom axes. Dot-dashed curves correspond to the previous quiet day. Positive latitude is north.

(Figure 3a, dashed curve 1 and dot-dashed curve Q); the increase reaches equatorial latitudes in 1.5 hours (in next orbit, data not shown) and becomes nearly equal at low and mid latitudes by the end of the MP (Figure 3a, solid curve 2). While N was decreasing during the short RP (data not shown), the next MP onset occurred. A similar development of the thermospheric storms (increase of N during MP and its decrease during RP) is repeated during the following two super storms (Figures 3b and 3c); the impulsive response at the MP onset of the Halloween storms (30 October 2003) produced the strongest TADs or travelling atmospheric disturbances (Figure 3c, dashed curve 5). Toward the end of the RP, N goes below quiet time levels (Figure 3d, curves 7, 8 and Q) before recovering [see also *Balan et al.*, 2011b].

4.2. Storm on 20–21 November 2003

4.2.1. Ionospheric Storms

[13] An independent super storm occurred on 20 November 2003 when CHAMP was crossing the 11.5 MLT meridian (Table 1, Figure 4). Though it is the most intense of all storms, it has fluctuations (in Dst) for the first 13 hours of the longest MP (18 hours). Figure 5 shows the development of ionospheric storms. As shown, a positive storm develops during early MP and covers all latitudes including the equator with the EIA crests shifting close to the equator (Figure 5a, dashed curve 1 and dot-dashed curve Q). With the progress of the MP the positive storm becomes weak except around the equator (data not shown). By the end of the MP there is a strong and sharp Ne peak (or positive storm) around the equator with large decreases of Ne (or severe negative storms) at higher latitudes (Figure 5a, solid curve 2). The positive storm around the equator continues during the RP (Figure 5b, dashed curve 3 and dot-dashed curve Q). Toward the end of the RP the ionosphere returns to quite-time levels with the development of EIA (Figure 5b, solid curve 4).

4.2.2. Thermospheric Storms

[14] Figure 6 shows the development of thermospheric storms. A comparatively weak thermospheric storm (increase of N) is found to start at high latitudes (data not shown) with the onset of the longest and most intense MP with fluctuations. The weak storm extends to low latitudes in about 7 hours (Figure 6a, dashed curve 1 and dot-dashed curve Q); it grows in strength and reaches peak levels by the end of the

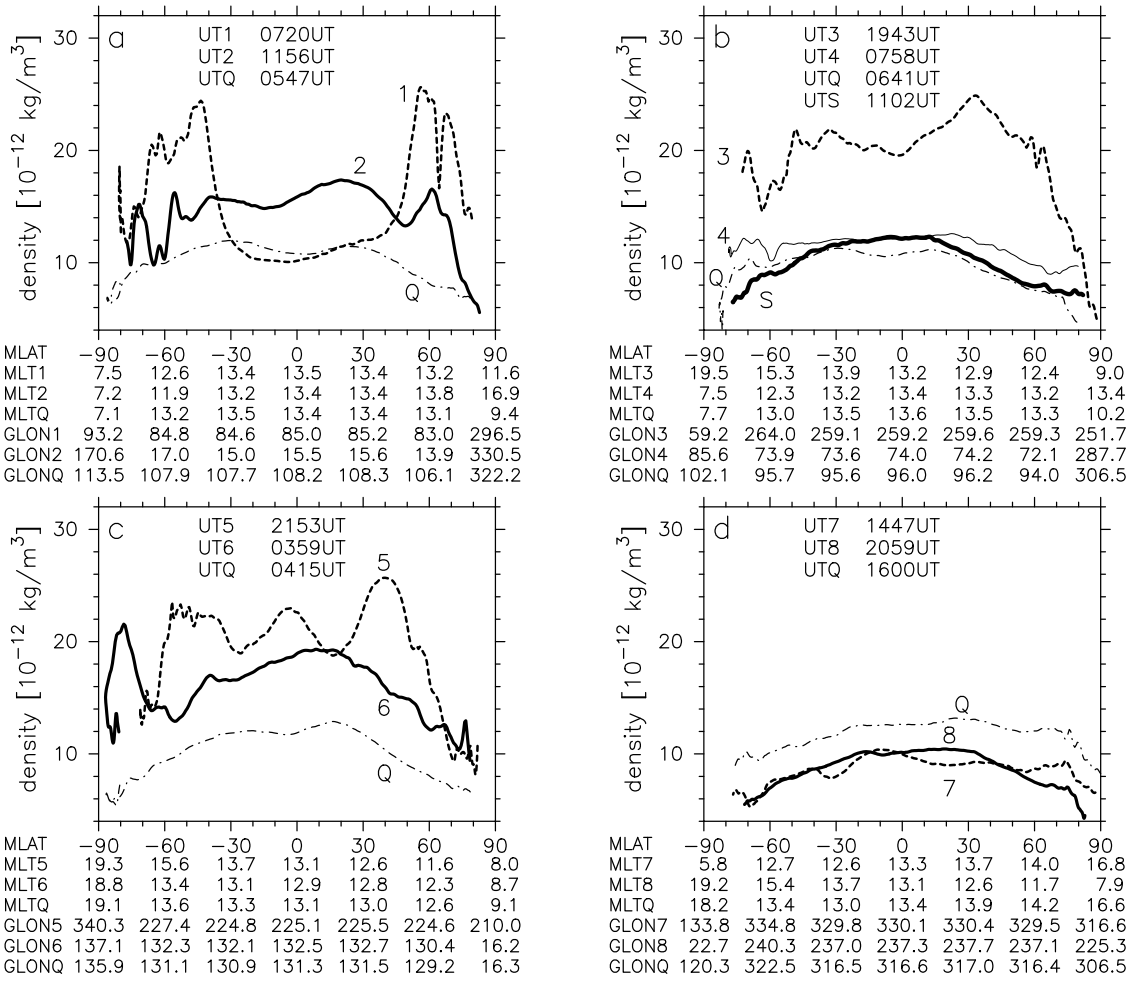

Figure 3. Same as Figure 2 but for neutral mass density N.

MP with a large summer to winter asymmetry (Figure 6a, solid curve 2). During RP, N decreases and reaches toward quiet time levels by the end of the RP (Figure 6b, curves 3, 4, Q).

4.3. Storm on 31 March to 1 April 2001

[15] A super double geomagnetic storm occurred on 31 March 2001 when CHAMP was crossing the 14.9 MLT meridian (Table 1 and Figure 7). As shown by Figures 8a

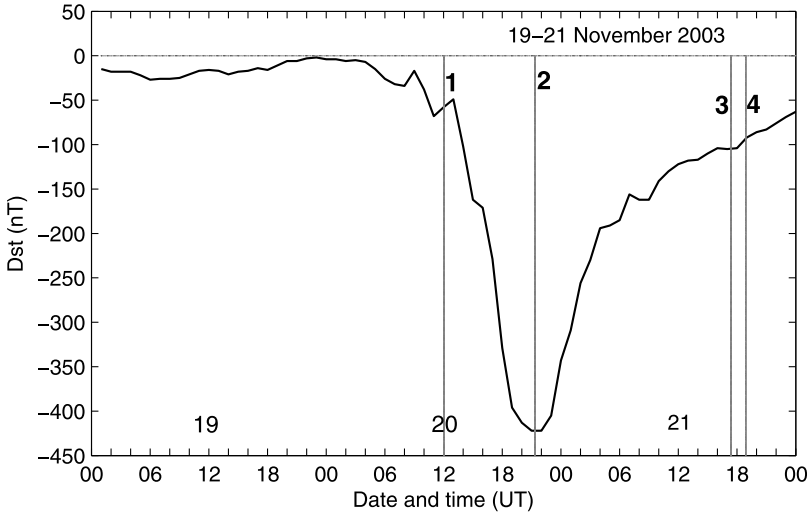

Figure 4. The geomagnetic storm of 20–21 November 2003; vertical lines represent the times when CHAMP data are shown in Figures 5 and 6.

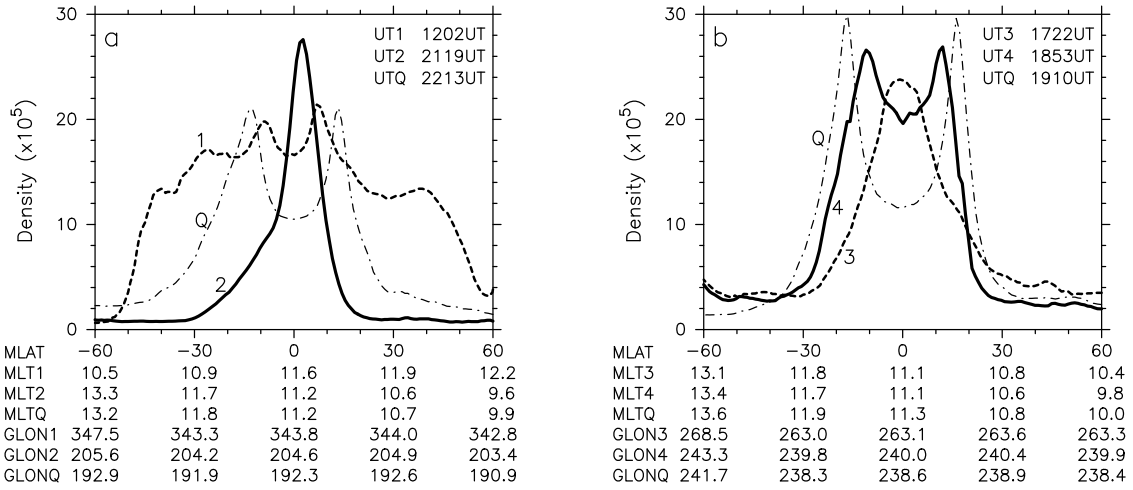

Figure 5. Latitude variations of the electron density Ne at selected equatorial crossing times of CHAMP during the superstorm of 20–21 November 2003. The satellite crossing times in UT (corresponding to the Ne plots) are noted at the top of the plots (and indicated by the vertical lines in Figure 4). The corresponding magnetic local times (MLT) and geographic longitudes (GLOG) are noted in the bottom axes. Dot-dashed curves correspond to the previous quiet day. Positive latitude is north.

and 8b, the Ne at equatorial latitudes during the RPs of both storms exceeds the quiet time levels (or produce positive ionospheric storms) though the positive storm during the first RP is asymmetric probably due to asymmetric neutral winds. However, the negative storm at equatorial latitudes and positive storm at higher latitudes in the north during the second MP appear weak (Figure 8b, curves 3 and Q); this is because the quiet time level corresponds to RP.

4.4. Storm on 10–13 August 2000

[16] Another double geomagnetic storm occurred on 10–13 August 2000 when CHAMP was crossing the 11.9 MLT meridian (Table 1 and Figure 9). During the MP of the first moderate storm, positive ionospheric storms develop outside the EIA trough with a small negative change inside the trough (Figure 10a, curves 1 and Q) indicating a weak eastward PPEF in the longitude of CHAMP. During RP, a positive storm develops centered over the equator with negative storms at higher latitudes (Figure 10a, curves 2 and Q). A similar development of ionospheric storms is repeated during the MP and RP of the re-intensified super storm (Figure 10b).

4.5. Further Data

[17] Four independent super storms occurred on 24–25 November 2001, 11–12 April 2001, 5–7 November 2001 and 7–8 November 2004 when CHAMP crossed the 17.6 MLT, 14.0 MLT, 19.5 MLT and 15 MLT respectively (Table 1 and Figure 11). In Figure 12 the data during MPs are shown in only one case (Figure 12a, dashed curve 1). Here we briefly describe the new aspect during the RPs. As shown by the comparison of Figures 11 and 12, positive ionospheric storms develop and continue at equatorial latitudes during the RPs of the super storms, with negative ionospheric storms at higher latitudes in all four cases. Figure 12 also shows an example of the change-over of the Ne pattern during MPs to that during RPs (Figure 12b, curve 1). The positive storms in Figure 12 are almost

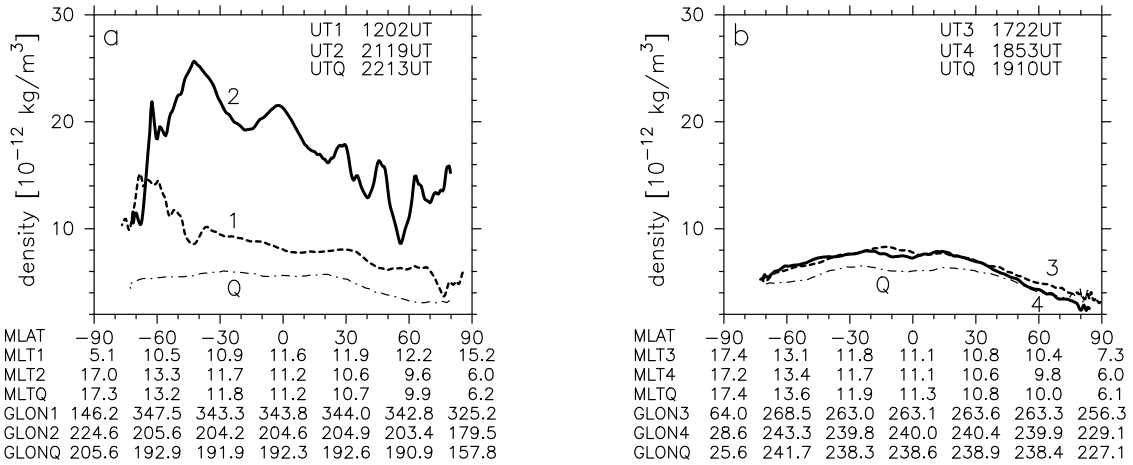

Figure 6. Same as Figure 5 but for neutral mass density N.

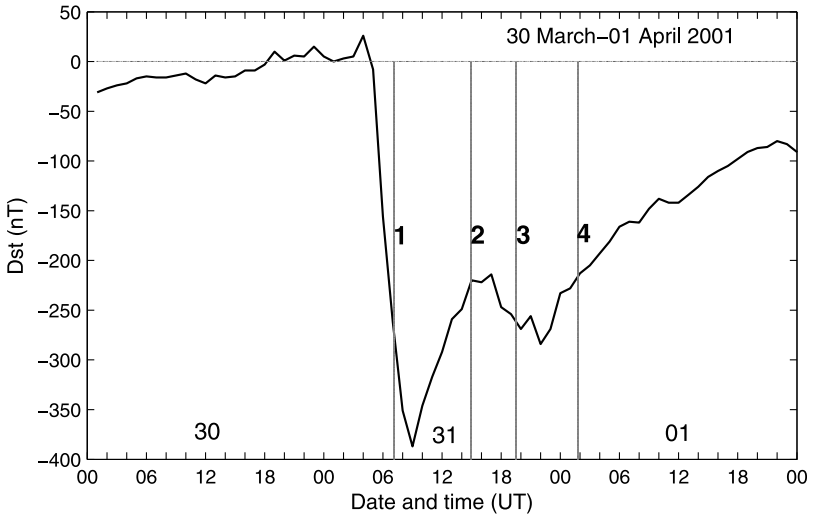

Figure 7. The double geomagnetic storm of 31 March to 1 April 2001; vertical lines represent the times when CHAMP data are shown in Figure 8.

symmetric with respect to the equator except on 6 November 2001 (Figure 12c, curves 1 and 2). This positive storm is detected in the 19.5 MLT meridian where the daytime production of ionization is absent; *C. M. Huang et al.* [2010] reported a similar case.

5. CHAMP, ROCSAT, and DMSP Observations

[18] Here we present the temporal evolution of the ionospheric storms and their altitude coverage. Figure 13 compares the ionospheric storms observed by CHAMP (400 km), ROCSAT (600 km) and DMSP (840 km) during the triple geomagnetic storm of 29–31 October 2003 (characteristics listed in Table 1). Figure 14 is similar to Figure 13 but for the single storm of 7–9 November 2004; ROCSAT data not available for this storm. The same colour scale is used for the same satellite data in Figures 13 and 14; the scale for ROCSAT is 33% less and DMSP is an order of magnitude less than that for CHAMP. Dayside data only are plotted; dayside longitudes crossed by the satellites are noted below the data sets; equatorial crossing times are noted in the caption. As shown by the data (Figures 13 and 14), ionospheric storms occur at all heights.

[19] During the storms on 29–31 October 2003 (Figure 13), compared to quiet time data (data before first MP), at CHAMP negative ionospheric storms develop at equatorial latitudes during part or whole of all three MPs due to eastward PPEFs, and positive storms occur at higher latitudes due to eastward PPEFs and equatorward neutral winds [e.g., *Mannucci et al.*, 2005; *Balan et al.*, 2011b]. During RPs, positive storms in general develop at equatorial latitudes while conventional negative storms occur at higher latitudes. However, the positive storms at equatorial latitudes are weak and asymmetric during early RPs, discussed in

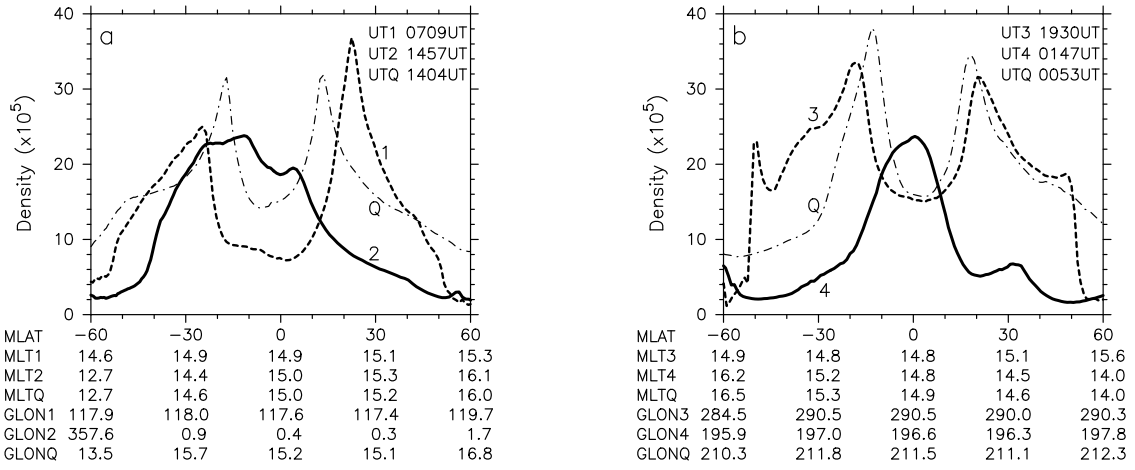

Figure 8. Latitude variations of the electron density Ne at selected equatorial crossing times of CHAMP during the double geomagnetic storm of 31 March to 1 April 2001. The satellite crossing times in UT (corresponding to the Ne plots) are noted at the top of the plots (and indicated by the vertical lines in Figure 7). The corresponding magnetic local times (MLT) and geographic longitudes (GLOG) are noted in the bottom axes. Dot-dashed curves correspond to the previous quiet day. Positive latitude is north.

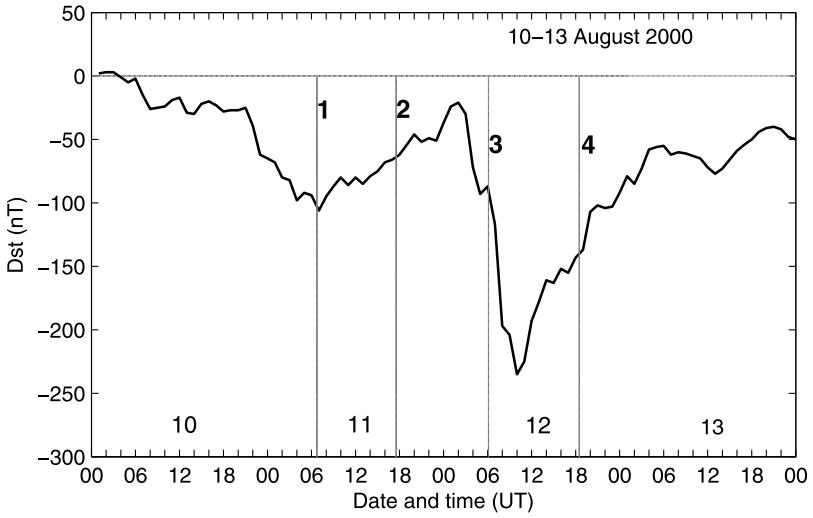

Figure 9. The double geomagnetic storm of 10–13 August 2000; vertical lines represent the times when CHAMP data are shown in Figure 10.

section 4.1. At DMSP (Figure 13), compared to quiet time levels, Ni is generally high especially during MPs. Hence, during MPs, positive storms occur in the topside ionosphere (at DMSP, 840 km height) while negative storms develop around the equatorial ionospheric peak (at CHAMP, 400 km height), discussed in section 6. At ROCSAT (600 km height), the ionospheric storms have characteristics more similar to those at CHAMP than at DMSP.

[20] During the super storm on 7–8 November 2004 (Figure 14), compared to quiet time levels, at CHAMP negative storms develop at equatorial latitudes with positive storms at higher latitudes during the MP. The pattern reverses during the RP. However, at DMSP, Ni is generally high especially during MP. As shown by the data (Figures 13 and 14), during MPs, the positive ionospheric storms are in general centered at around ±30° magnetic latitudes at 400 km height, and the storm centers shift close the equator at higher heights as expected from a physical mechanism of the positive storms [*Balan et al.*, 2010, 2011b]. However, the positive storms during the MP on 30 October 2003 (Figure 13) extend to the southern sub-auroral latitudes indicating contributions from intense sub-auroral electric fields [*Foster*, 1993; *Heelis et al.*, 2009].

6. Discussion

[21] The most important features identified from this study during the 12 intense geomagnetic storms are outlined and discussed in this section. CHAMP Ne (section 4) data revealed the development of positive ionospheric storms at equatorial latitudes during daytime RPs (new aspect). As listed in Table 1 and shown by the data, the positive storms

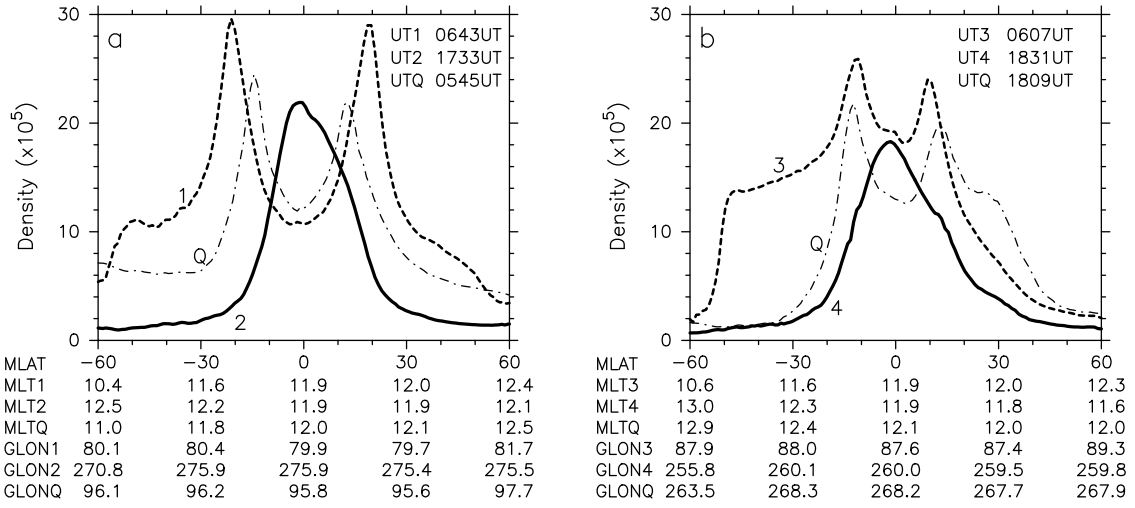

Figure 10. Latitude variations of the electron density Ne at selected equatorial crossing times of CHAMP during the double geomagnetic storms of 10–13 August 2000. The satellite crossing times in UT (corresponding to the Ne plots) are noted at the top of the plots (and indicated by the vertical lines in Figure 9). The corresponding magnetic local times (MLT) and geographic longitudes (GLOG) are noted in the bottom axes. Dot-dashed curves correspond to the previous quiet day. Positive latitude is north.

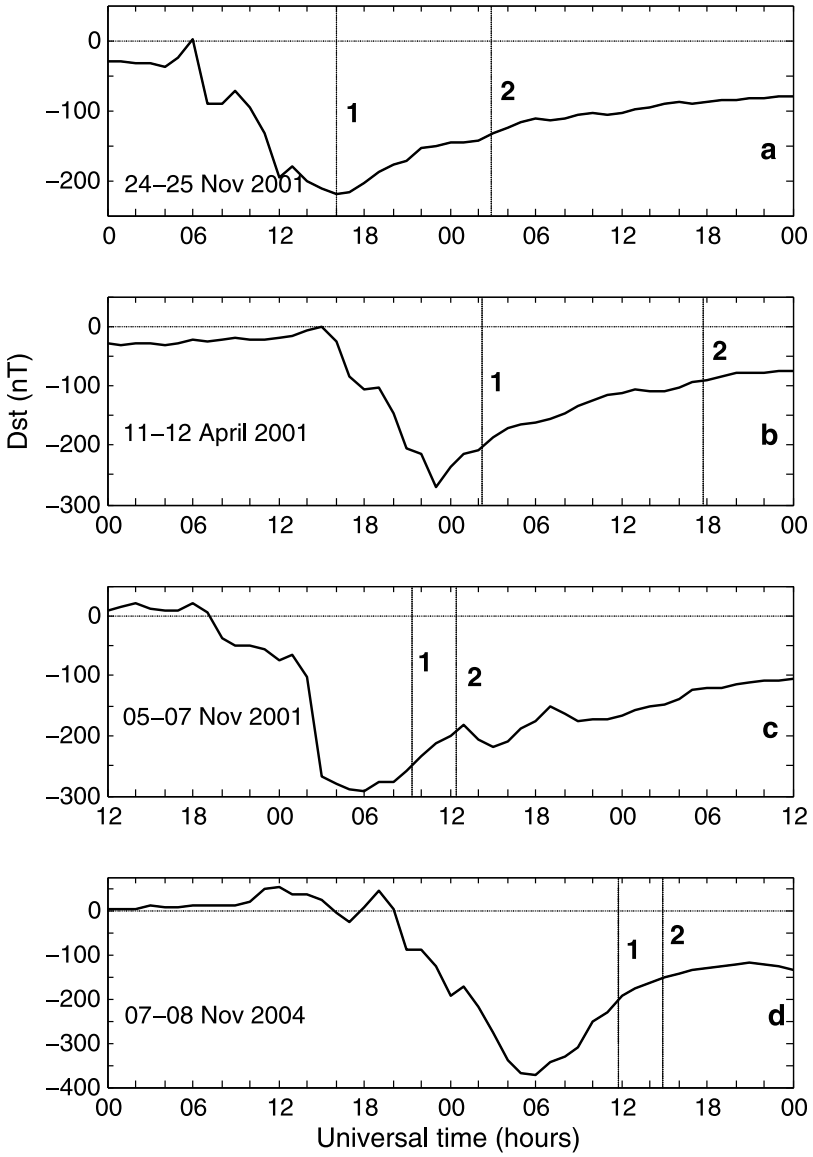

Figure 11. The single geomagnetic storms of (a) 24–25 November 2001, (b) 11–12 April 2001, (c) 5–7 November 2001, and (d) 7–8 November 2004; vertical lines represent the times when CHAMP data are shown in Figure 12.

at equatorial latitudes during daytime RPs seem to occur irrespective of the local time, longitude, season and solar activity levels of the RPs. CHAMP, ROCSAT and DMSP data (section 5) showed the ionospheric storms extending to the topside ionosphere beyond 850 km. However, unlike near the ionospheric peak (at CHAMP), the ionospheric storms in the topside ionosphere at DMSP (840 km) are generally positive especially during MPs. Here we discuss the physical mechanisms of the new aspects. The potential sources of the positive storms during RP include (1) zero or westward electric fields due to prompt penetration and/or disturbance dynamo, (2) plasma convergence due to the mechanical effect of storm-time equatorward winds and waves, (3) increase of atomic oxygen density [O] and decrease of molecular nitrogen density [N_2] due to the downwelling (chemical) effect of the equatorward winds, and photoionization. Whereas, the positive storms in the topside ionosphere (at DMSP) during the MPs involve the rapid upward drift of plasma due to eastward PPEFs, reduction in downward diffusion of plasma along the field lines and plasma convergence due to equatorward winds.

6.1. Zero or Westward Electric Fields

[22] The net electric field over the equator during part or whole of the dayside RPs generally remains null or westward due to the disturbance dynamo and/or prompt penetration [*Blanc and Richmond*, 1980; *Kelley et al.*, 2003; *Maruyama et al.*, 2005; *Fejer et al.*, 2007; *C. S. Huang et al.*, 2010; *Balan et al.*, 2010]. When the electric field is zero, the removal of plasma from around the equator by the forward fountain ceases. Hence the latitude variation of Ne (at CHAMP) and Nmax can peak over the equator due to

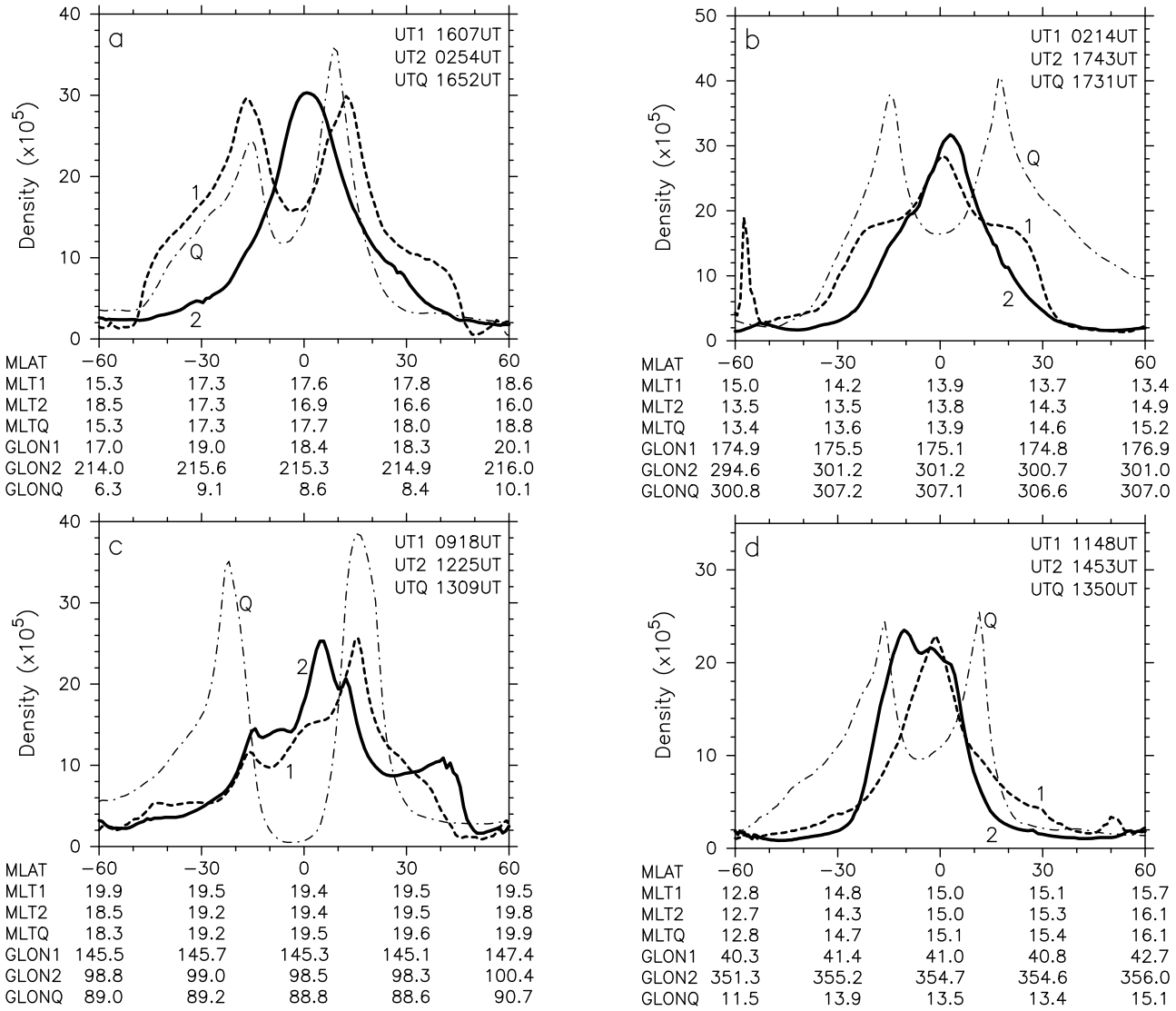

Figure 12. Latitude variations of the electron density Ne at selected equatorial crossing times of CHAMP during the single geomagnetic storms of (a) 24–25 November 2001, (b) 11–12 April 2001, (c) 5–7 November 2001, and (d) 7–8 November 2004. The satellite crossing times in UT (corresponding to the Ne plots) are noted at the top of each plot (and indicated by the vertical lines in Figure 11). The corresponding magnetic local times (MLT) and geographic longitudes (GLOG) are noted in the bottom axes. Dot-dashed curves correspond to the previous quiet day. Positive latitude is north.

the daytime production of ionization. The situation is similar to what *Namba and Maeda* [1939] and *Appleton* [1946] might have expected before they discovered the EIA. If the electric field is westward, the resulting downward $\mathbf{E} \times \mathbf{B}$ drift compresses the equatorial F region vertically downward, which further increases Ne and Nmax. At the same time, the inward $\mathbf{E} \times \mathbf{B}$ drift at higher latitudes largely reduces Ne and Nmax because the drift accelerates the downward diffusion of plasma and also lowers the ionosphere to low altitudes of increased chemical loss. The results are sharper Ne and Nmax peaks at equatorial latitudes than when the net electric field is zero. In both cases the EIA is inhibited as reported by *Pincheira et al.* [2002], *Tulasi Ram et al.* [2008], *Sreeja et al.* [2009b], and *C. M. Huang et al.* [2010].

6.2. Mechanical Effects of Storm-Time Equatorward Winds

[23] Storm-time equatorward surges, TADs, and winds (of velocity U) from both poles reach the equator soon after the onset of geomagnetic storms with steady MPs (within 1.5 to 3 hours) and continue during RPs (section 4, Figures 3 and 6) [*Prölss and Jung*, 1978; *Fuller Rowell et al.*, 1994]. One of the mechanical effects of the winds (proportional to $UcosI$ with I being dip angle) reduces the downward diffusion of plasma along the field lines, which maximizes over the equator ($I = 0$) (where diffusion is minimum) [*Balan et al.*, 2010]. Since this effect accumulates the plasma along the field lines (from the point of interaction between the field line and wind), the plasma converges over the equator when the winds from both hemispheres reach the equator. The

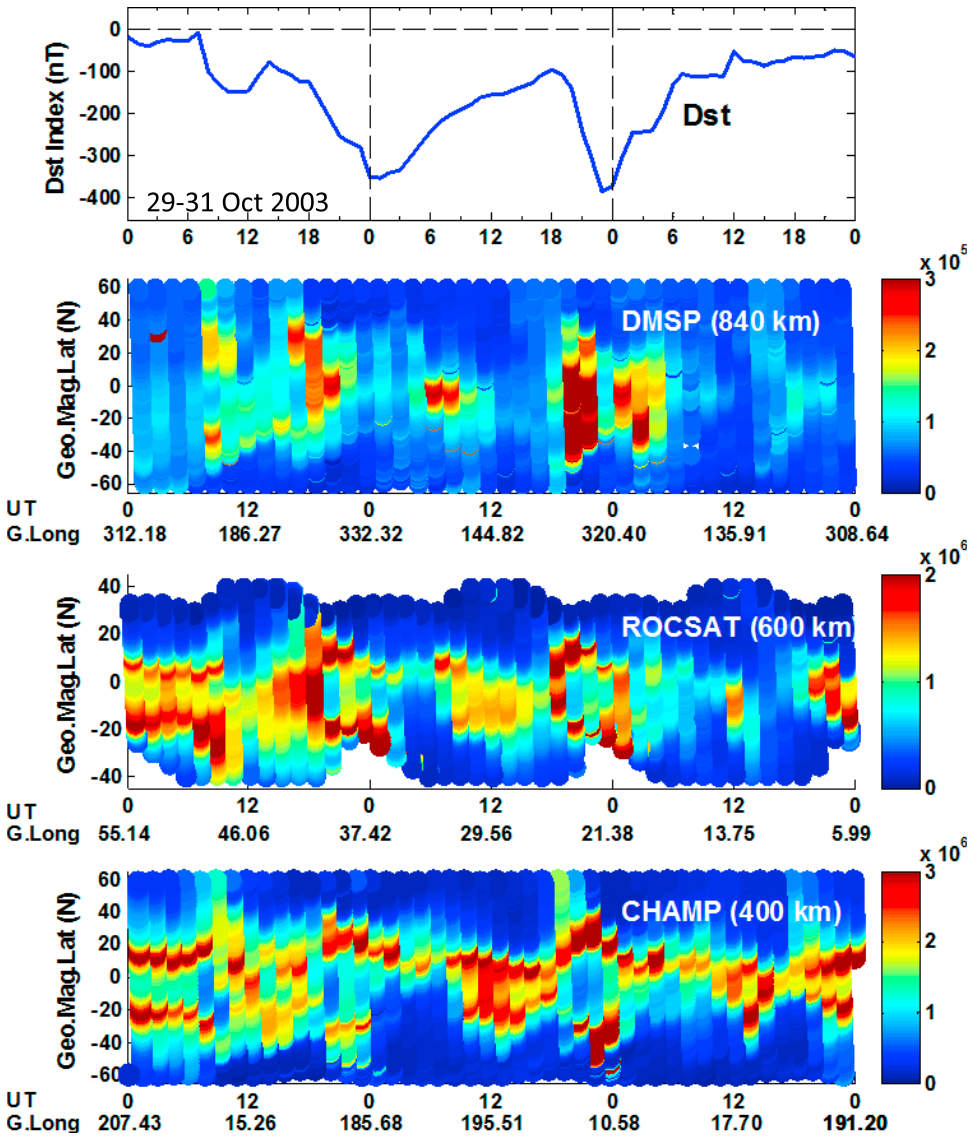

Figure 13. Latitude verses time (UT) plots of the daytime (06:00–18:00 LT) electron density at 400 km height measured by CHAMP, daytime ion density at 600 km height measured by ROCSAT, and daytime ion density at 840 km height measured by DMSP F15 during the triple geomagnetic storm of 29–31 October 2003. The equatorial crossing longitudes of the satellites are noted below the data set; the equatorial crossing local times are approximately 13:01 LT (CHAMP), 12:55 LT (ROCSAT), and 09:48 LT (DMSP). Positive latitude is north.

other mechanical effect (proportional to *UcosIsinI*) can slightly rise the F region peak at equatorial locations where geomagnetic and geographic equators do not coincide as in most places. The mechanical effects of the winds can therefore cause sharp peaks in Ne at all heights over the equator.

6.3. Downwelling Effect of Storm-Time Equatorward Winds

[24] The expansion (or upwelling) of the thermosphere due to high latitude heating during geomagnetic storms largely reduces the $[O]/[N_2]$ ratio at mid and low latitudes [e.g., *Prölss*, 1995]. When the resulting equatorward winds reach the equator their downwelling can increase the $[O]/[N_2]$ ratio around the equator [*Roble et al.*, 1982] as observed by GUVI [*Meier et al.*, 2005]. The downwelling can therefore produce Ne (at CHAMP) and Nmax peaks at equatorial latitudes due to increased daytime production and reduced chemical loss of ionization. At the same time (during late MPs and RPs), the Ne and Nmax at higher latitudes undergo severe negative ionospheric storms due to the large decrease of $[O]/[N_2]$ [e.g., *Prölss*, 1995]. Recently, using TIMED/GUVI observations *Kil et al.* [2011] reported an increase of [O] and decrease of $[N_2]$ (or increase of $[O]/[N_2]$) around the equator during the late MP of the 20 November 2003 geomagnetic storm when a sharp Ne peak is observed by CHAMP (Figure 5).

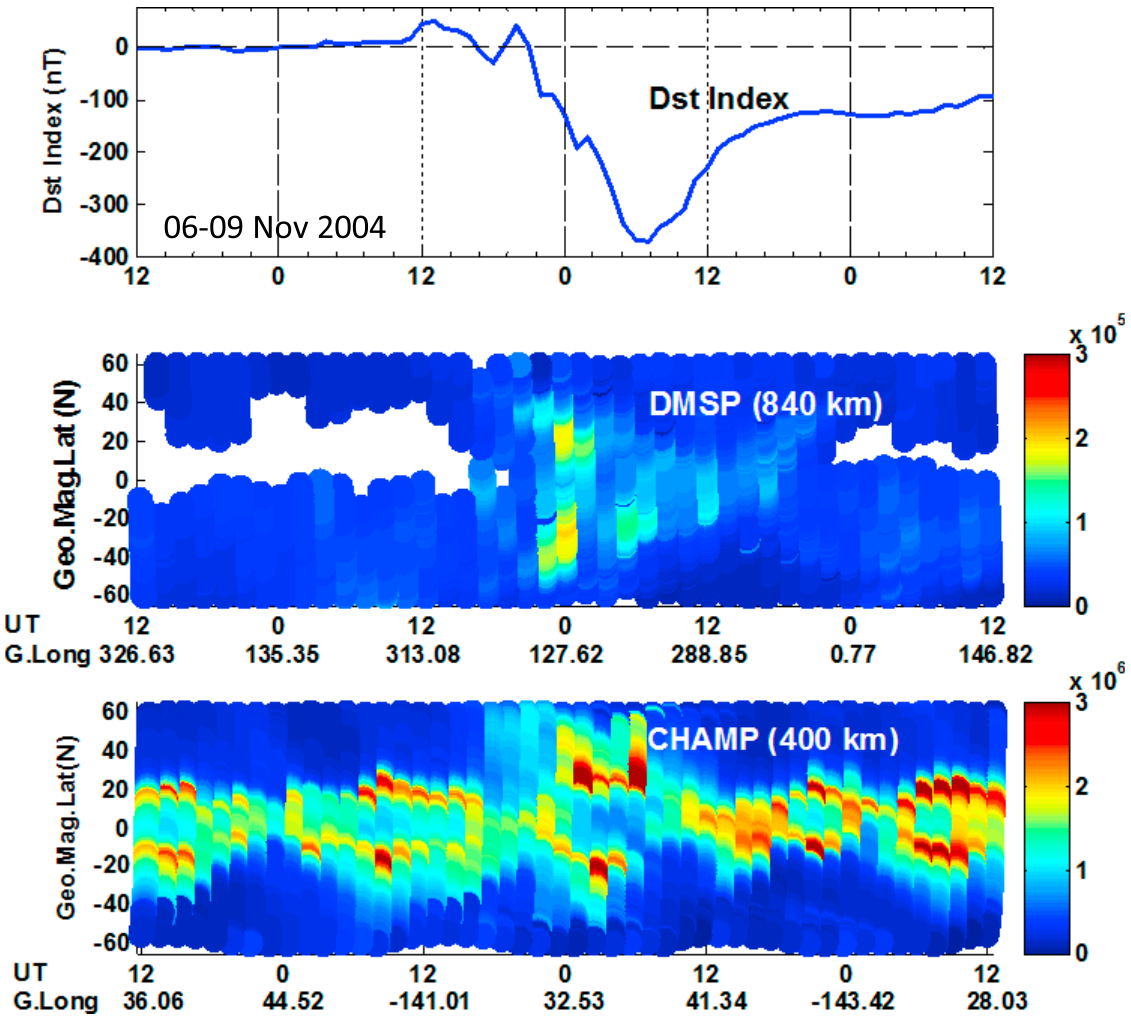

Figure 14. Latitude verses time (UT) plots of the daytime (06:00–18:00 LT) electron density at 400 km height measured by CHAMP and daytime ion density at 840 km height measured by DMSP F15 during the geomagnetic storm of 7–9 November 2004. The equatorial crossing longitudes of the satellites are noted below the data set; the equatorial crossing local times are approximately 14:34 LT (CHAMP) and 09:19 LT (DMSP). Positive latitude is north.

6.4. Upward Drift Due to Eastward PPEFs

[25] Eastward PPEFs of varying strengths occur during part or whole of the MPs of all geomagnetic storms [*Tsurutani et al.*, 2004; *Maruyama et al.*, 2005; *Fejer et al.*, 2007; *Abdu et al.*, 2008; *C. S. Huang et al.*, 2010; *Balan et al.*, 2011a]. The PPEFs rapidly drift the plasma from around the equatorial ionospheric peak (at CHAMP and ROCSAT) to the topside ionosphere (at DMSP) [e.g., *Balan et al.*, 2009] where the electric field is comparatively weak [e.g., *Fejer et al.*, 2007; *C. S. Huang et al.*, 2010]. Then, from the topside equatorial ionosphere, the downward diffusion of plasma along the field lines becomes weak due to the horizontal orientation of the field lines; the decrease in the plasma pressure difference along the field lines due to the positive storms (in Nmax and TEC) at higher latitudes also reduces the downward diffusion. These together with the plasma convergence (discussed in mechanism 2 above) due to storm-time equatorward winds that remain constant at altitudes near and above the ionospheric peak [e.g., *Hedin et al.*, 1991] can cause positive ionospheric storms in the topside ionosphere (at DMSP) during MPs.

[26] The thermospheric storms (change of N) originating at high latitudes reach the equator faster for geomagnetic storms with short and steady MPs than for storms with long and fluctuating MPs (section 4, Figures 3 and 6) [*Fuller Rowell et al.*, 1994; *Balan et al.*, 2011b]. For example, the thermospheric storms on 29 October 2003 (minimum Dst = −151 nT, MP duration 4 hours) and on 30 October 2003 (minimum Dst = −383 nT, MP duration 5 hours) reach the equator within 1.5 to 3 hours (the uncertainty is due to the orbital period of 1.5 hours). However, the thermospheric storms on 20 November 2003 (minimum Dst =−422 nT, MP duration 18 hours with fluctuations) reach the equator about 7 hours after MP onset; similar is the case for the second MP onset on 29 October 2003.

[27] The sources discussed above (independently or together) can produce Ne, Nmax and TEC peaks (or positive storms) at equatorial latitudes during daytime RPs when conventional negative ionospheric storms occur at higher

latitudes as observed. The equatorial peaks can be displaced to one side of the equator (where the $[O]/[N_2]$ ratio is high) when the neutral wind becomes asymmetric. It is also possible for the negative ionospheric storms at mid and low latitudes to extend to the equator, which can cause delayed and asymmetric development of the positive storms in some cases as during the supper storms on 29–30 October 2003 and 31 March to 1 April 2001 (sections 4.1 and 4.3). In all cases, the ionosphere returns to quite-time levels with the development of EIA by the end of RPs. The rapid upward drift of plasma due to eastward PPEFs, reduction in the downward diffusion of plasma along the field lines, and convergence effect of equatorward neutral winds and waves can produce positive storms in Ne in the topside ionosphere especially during MPs. Model results investigating the relative effects of the different sources will be presented in a later paper for different storm scenarios.

7. Conclusions

[28] The neutral mass density (N) and electron density (Ne) at 400 km height measured by CHAMP during 12 intense geomagnetic storms in 2000–2004, and the ion densities at 600 km and 840 km heights measured by ROSCAT and DMSP during a few of the intense storms reveal some new aspects. Thermospheric storms (change of N) reach the equator within 1.5 to 3 hours from the main phase (MP) onset of intense storms having short and steady MPs. In addition to the known opposite responses of the equatorial and higher latitude ionospheres during daytime MPs, the analysis reveals that positive ionospheric storms develop around the equatorial ionospheric peak (at CHAMP) during daytime RPs (recovery phases) while conventional negative storms occur at higher latitudes. The positive storms during RPs could be caused by (1) zero or westward electric fields due to disturbance dynamo and/or prompt penetration, (2) plasma convergence due to the mechanical effects of storm-time equatorward neural winds and waves, (3) increase of atomic oxygen density and decrease of molecular nitrogen density due to the downwelling of equatorward winds, and photoionization. In addition, ionospheric storms extend to the topside ionosphere beyond 850 km height and are generally positive (at DMSP) especially during MPs. This involves the upward drift of plasma due to eastward PPEFs, reduction in the downward diffusion of plasma along the field lines and plasma convergence due to equatorward winds and waves. However, the development of the positive storms at CHAMP during the RPs of the Halloween storms (29–30 October 2003) is delayed due to the deep and wide depletions of Ne during the MPs and extension of the negative storms in the south to the equator during early RPs. The study suggests the need to monitor the ionospheric electric fields and thermospheric neutral winds and composition to understand the ionospheric storms that can cause serious problems in power supply systems, satellite systems, and satellite navigation and communication.

[29] **Acknowledgments.** N. Balan thanks the Institute of Space Science of National Central University (Taiwan) for providing a visiting professor position. We thank the National Science Council (NSC) of Taiwan for grants NSC98-2111-M-008-008-MY3 and NSC100-2811-M-008-034, under which this work is carried out. The work of Tulasi Ram is supported by the JSPS Foundation. The CHAMP mission is supported by the German Aerospace Center (DLR) in operation, and by the Federal Ministry of Education and Research (BMBF) in data processing. The ROCSAT-1 mission is supported by NSPO, Taiwan, and data are provided by National Central University (NCU) through http://csrsddc.csrsr.ncu.edu.tw/Welcome.html. The Center for Space Science at the University of Texas at Dallas and U.S. Air Force provided the DMSP data.

[30] Robert Lysak thanks the reviewers for their assistance in evaluating this paper.

References

Abdu, M. A., et al. (2008), Abnormal evening vertical plasma drift and effects on ESF and EIA over Brazil–South Atlantic sector during the 30 October 2003 superstorm, *J. Geophys. Res.*, *113*, A07313, doi:10.1029/2007JA012844.

Appleton, E. V. (1946), Two anomalies in the ionosphere, *Nature*, *157*, 691.

Balan, N., and P. B. Rao (1990), Dependence of ionospheric response on the local time of sudden commencement and intensity of storms, *J. Atmos. Terr. Phys.*, *52*, 269.

Balan, N., K. Shiokawa, Y. Otsuka, S. Watanabe, and G. J. Bailey (2009), Super plasma fountain and equatorial ionization anomaly during penetration electric field, *J. Geophys. Res.*, *114*, A03310, doi:10.1029/2008JA013768.

Balan, N., K. Shiokawa, Y. Otsuka, T. Kikuchi, D. Vijaya Lekshmi, S. Kawamura, M. Yamamoto and G. J. Bailey (2010), A physical mechanism of positive ionospheric storms at low latitudes and midlatitudes, *J. Geophys. Res.*, *115*, A02304, doi:10.1029/2009JA014515.

Balan, N., et al. (2011a), A statistical study of the response of the dayside equatorial F2 layer to the main phase of intense geomagnetic storms as an indicator of penetration electric field, *J. Geophys. Res.*, *116*, A03323, doi:10.1029/2010JA016001.

Balan, N., M. Yamamoto, J. Y. Liu, Y. Otsuka, H. Liu, and H. Lühr (2011b), New aspects of thermospheric and ionospheric storms revealed by CHAMP, *J. Geophys. Res.*, *116*, A07305, doi:10.1029/2010JA016399.

Batista, I. S., E. de Paula, M. A. Abdu, N. Trivedi, and M. Greenspan (1991), Ionospheric effects of the March 13, 1989, magnetic storm at low and equatorial latitudes, *J. Geophys. Res.*, *96*(A8), 13,943.

Blanc, M., and A. Richmond (1980), The ionospheric disturbance dynamo, *J. Geophys. Res.*, *85*(A4), 1669–1686.

Burns, A. G., T. L. Killeen, W. Deng, G. R. Carignan, and R. G. Roble (1995), Geomagnetic storm effects in the low- to middle-latitude upper thermosphere, *J. Geophys. Res.*, *100*, 14,673.

Fejer, B. G., J. W. Jensen, T. Kikuchi, M. A. Abdu, and J. L. Chau (2007), Equatorial ionospheric electric fields during the November 2004 magnetic storm, *J. Geophys. Res.*, *112*, A10304, doi:10.1029/2007JA012376.

Foster, J. C. (1993), Storm-time plasma transport at middle and high latitudes, *J. Geophys. Res.*, *98*, 1675–1689.

Fuller-Rowell, T. J., M. V. Codrescu, R. J. Moffett, and S. Quegan (1994), Response of the thermosphere and ionosphere to geomagnetic storms, *J. Geophys. Res.*, *99*, 3893.

Hanson, W. B., and R. J. Moffett (1966), Ionization transport effects in the equatorial F region, *J. Geophys. Res.*, *71*, 5559.

Hedin, A. E., et al. (1991), Revised global model of thermosphere winds using satellite and ground-based observations, *J. Geophys. Res.*, *96*, 7657.

Heelis, R. A., J. J. Sojka, M. David, and R. W. Schunk (2009), Storm time density enhancements in the midlatitude dayside ionosphere, *J. Geophys. Res.*, *114*, A03315, doi:10.1029/2008JA013690.

Huang, C. M., M. Q. Chen, and J. Y. Liu (2010), Ionospheric positive storm phases at the magnetic equator close to sunset, *J. Geophys. Res.*, *115*, A07315, doi:10.1029/2009JA014936.

Huang, C. S., F. J. Rich, and W. J. Burke (2010), Storm time electric fields in the equatorial ionosphere near the dusk meridian, *J. Geophys. Res.*, *115*, A08313, doi:10.1029/2009JA015150.

Kelley, M. C., J. J. Mekela, J. L. Chau, and M. J. Nicolls (2003), Penetration of solar wind electric field into the magnetosphere/ionosphere system, *Geophys. Res. Lett.*, *30*(4), 1158, doi:10.1029/2002GL016321.

Kelley, M. C., M. N. Vlasov, J. C. Foster, and A. J. Coster (2004), A quantitative explanation for the phenomenon known as storm-enhanced density, *Geophys. Res. Lett.*, *31*, L19809, doi:10.1029/2004GL020875.

Kikuchi, T., T. Araki, H. Maeda, and K. Maekawa (1978), Transmission of polar electric fields to the equator, *Nature*, *273*, 650–651.

Kil, H., Y.-S. Kwak, L. J. Paxton, R. R. Meier, and Y. Zhang (2011), O and N_2 disturbances in the F region during the 20 November 2003 storm seen from TIMED/GUVI, *J. Geophys. Res.*, *116*, A02314, doi:10.1029/2010JA016227.

Lei, J., J. P. Thayer, A. G. Burns, G. Lu, and Y. Deng (2010), Wind and temperature effects on thermosphere mass density response to the November 2004 geomagnetic storm, *J. Geophys. Res.*, *115*, A05303, doi:10.1029/2009JA014754.

Lin, C. H., A. D. Richmond, R. A. Heelis, G. J. Bailey, G. Lu, J. Y. Liu, H. C. Yeh, and S. Y. Su (2005), Theoretical study of the low and mid-latitude ionospheric electron density enhancement during the October 2003 storm: Relative importance of the neutral wind and the electric field, *J. Geophys. Res.*, *110*, A12312, doi:10.1029/2005JA011304.

Liu, H., and H. Lühr (2005), Strong disturbance of the thermospheric density due to storms: CHAMP observations, *J. Geophys. Res.*, *110*, A09S29, doi:10.1029/2004JA010908.

Liu, H., H. Lühr, V. Henize, and W. Köhler (2005), Global distribution of the thermospheric density derived from CHAMP, *J. Geophys. Res.*, *110*, A04301, doi:10.1029/2004JA010741.

Liu, R., H. Lühr, E. Doornbos, and S.-Y. Ma (2010), Thermospheric mass density variations during geomagnetic storms and a prediction model based on the merging electric field, *Ann. Geophys.*, *28*, 1633–1645.

Lu, G., L. P. Goncharenko, A. D. Richmond, R. G. Roble, and N. Aponte (2008), A dayside ionospheric positive storm phase driven by neutral winds, *J. Geophys. Res.*, *113*, A08304, doi:10.1029/2007JA012895.

Mannucci, A. J., B. T. Tsurutani, B. A. Iijima, A. Komjathy, A. Saito, W. D. Gonzalez, F. L. Guarnieri, J. U. Kozyra, and R. Skoug (2005), Dayside global ionospheric response to the major interplanetary events of October 29–30, 2003 "Halloween Storms,"*Geophys. Res. Lett.*, *32*, L12S02, doi:10.1029/2004GL021467.

Maruyama, N., A. D. Richmond, T. J. Fuller-Rowell, M. V. Coderscu, S. Sazykin, F. R. Toffoletto, R. W. Spiro, and G. H. Millward (2005), Interaction between direct penetration and disturbance dynamo electric fields in the storm-time equatorial ionosphere, *Geophys. Res. Lett.*, *32*, L17105, doi:10.1029/2005GL023763.

Meier, R., G. Crowley, D. J. Strickland, A. B. Christensen, L. J. Paxton, D. Morrison, and C. L. Hackert (2005), First look at the 20 November 2003 superstorm with TIMED/GUVI: Comparisons with a thermospheric global circulation model, *J. Geophys. Res.*, *110*, A09S41, doi:10.1029/2004JA010990.

Mendillo, M., and C. Narvaez (2010), Ionospheric storms at geophysically equivalent sites: Part 2. Local time patterns for sub-auroral ionospheres, *Ann. Geophys.*, *28*, 1449.

Namba, S., and K.-I. Maeda (1939), *Radio wave propagation, report*, p. 86, Corona, Tokyo.

Paznukhov, V. V., B. W. Reinisch, P. Song, X. Huang, T. W. Bullett and O. Veliz (2007), Formation of an F_3 layer in the equatorial ionosphere: A result from strong IMF changes, *J. Atmos. Sol. Terr. Phys.*, *69*, 1292, doi:10.1016/j.jastp.2006.08.019.

Pincheira, X. T., M. A. Abdu, I. S. Batista, and P. G. Richards (2002), An investigation of ionospheric responses, and disturbance thermospheric winds, during magnetic storms over South America sector, *J. Geophys. Res.*, *107*(A11), 1379, doi:10.1029/2001JA000263.

Prölss, G. W. (1995), Ionospheric F region storms, in *Handbook of Atmospheric Electrodynamics*, edited by H. Volland, pp. 195–248, CRC Press, Boca Raton, Fla.

Prölss, G. W., and M. J. Jung (1978), Traveling atmospheric disturbances as a possible explanation for daytime positive storm effects of moderate duration at middle latitudes, *J. Atmos. Terr. Phys.*, *40*, 1351.

Rajaram, G. (1977), Structure of the equatorial F region, topside and bottomside: A review, *J. Atmos. Terr. Phys.*, *39*, 1125.

Rastogi, R. G. (1977), Geomagnetic storms and electric fields in the equatorial ionosphere, *Nature*, *268*, 422.

Reigber, C., H. Lühr, and P. Schwintzer (2002), CHAMP mission status, *Adv. Space Res.*, *30*, 129–134.

Rishbeth, H. (2000), The equatorial F region: Progress and puzzles, *Ann. Geophy.*, *18*, 730.

Roble, R. G., R. E. Dickinson, and E. C. Ridley (1982), Global circulation and temperature structures of thermosphere with high-latitude convection, *J. Geophys. Res.*, *87*, 1599.

Sastri, J., N. Jyoti, V. Somayajulu, H. Chandra, and C. Devasia (2000), Ionospheric storm of early November 1993 in the Indian equatorial region, *J. Geophys. Res.*, *105*(A8), 18,443.

Sreeja, V., N. Balan, S. Ravindran, T. K. Pant, R. Sridharan, and G. J. Bailey (2009a), Additional stratifications in the equatorial F region at dawn and dusk during geomagnetic storms: Role of electrodynamics, *J. Geophys. Res.*, *114*, A08309, doi:10.1029/2009JA014373.

Sreeja, V., S. Ravindran, T. K. Pant, C. V. Devasia, and L. J. Paxton (2009b), Equatorial and low-latitude ionosphere-thermosphere system response to the space weather event of August 2005, *J. Geophys. Res.*, *114*, A12307, doi:10.1029/2009JA014491.

Su, S. Y., H. C. Yeh, R. A. Heelis, J. M. Wu, S. C. Yang, L. F. Lee, and H. L. Chen (1999), The ROCSAT-1 IPEI preliminary results: Low-latitude ionospheric plasma and flow variations, *Terr. Atmos. Oceanic Sci.*, *10*, 787–804.

Sutton, E. K., J. M. Forbes, and R. S. Nerem (2005), Global thermospheric neutral density and wind response to the severe 2003 geomagnetic storms from CHAMP accelerometer data, *J. Geophys. Res.*, *110*, A09S40, doi:10.1029/2004JA010985.

Tsurutani, B., et al. (2004), Global ionospheric uplift and enhancement associated with interplanetary electric fields, *J. Geophys. Res.*, *109*, A08302, doi:10.1029/2003JA010342.

Tulasi Ram, S., P. V. S. Rama Rao, D. S. V. V. D. Prasad, K. Niranjan, S. Gopi Krishna, R. Sridharan, and S. Ravindran (2008), Local time dependent response of postsunset ESF during geomagnetic storms, *J. Geophys. Res.*, *113*, A07310,doi:10.1029/2007JA012922.

Tulasi Ram, S., S.-Y. Su, C. H. Liu, B. W. Reinisch and L.-A. McKinnell (2009), Topside ionospheric effective scale heights (H_T) derived from ROCSAT-1 and ground-based Ionosonde observations at equatorial and midlatitude stations, *J. Geophys. Res.*, *114*, A10309, doi:10.1029/2009JA014485.

Vijaya Lekshmi, D., N. Balan, V. K. Vaidyan, H. Alleyne, and G. J. Bailey (2007), Response of the ionosphere to super storms, *Adv. Space Res.*, *41*, 548–555, doi:/10.1016/j.asr.2007.08.029.

Yeh, H. C., S. Y. Su, Y. C. Yeh, J. M. Wu, R. A. Heelis and B. J. Holt (1999), Scientific mission of the IPEI payload onboard ROCSAT-1, *Terr. Atmos. Oceanic Sci.*, suppl., 19–42.

N. Balan and J. Y. Liu, Institute of Space Science, National Central University, Chung-Li, Taiwan. (b.nanan@sheffield.ac.uk)

H. Lühr, GFZ, German Research Centre for Geosciences, D-14473 Potsdam, Germany.

Y. Otsuka, Solar-Terrestrial Environment Laboratory, Nagoya University, Nagoya 464-8601, Japan.

S. Tulasi Ram, Research Institute for Sustainable Humanosphere, Kyoto University, Kyoto 611-0011, Japan.